Current Research in Food Science 4 (2021) 250–261

Contents lists available at ScienceDirect

Current Research in Food Science

journal homepage: www.editorialmanager.com/crfs/

Research Paper

A semi dynamic *in vitro* digestion study of milk protein concentrate dispersions structured with different polysaccharides

Jacob Østergaard Markussen [a,b], Finn Madsen [b,1], Jette Feveile Young [a], Milena Corredig [a,*,1]

[a] Department of Food Science, CiFood Multidisciplinary Center, Aarhus University, 48 Agro Food Park, Aarhus N, 8200, Denmark
[b] IFF R&D Braband, DuPont Nutrition Biosciences ApS, Edwin Rahrs Vej 38, 8220, Brabrand, Denmark

ARTICLE INFO

Keywords:
Hydrocolloids
In vitro digestion
Semi-dynamic
Milk protein concentrate
Food matrix

ABSTRACT

Hydrocolloids are often added as functional ingredients in foods, to better design the structure of the matrix and ensure food quality and optimal sensory properties. However, much less is known about their influence on the physical and chemical changes during gastric digestion. In this study, semi-continuous *in vitro* gastric digestion was applied on a model food system, prepared with milk protein concentrate (MPC) (3% w/v) and 1% alginate, pectin, guar gum, as well as a 1:1 mixture of alginate and pectin. The dynamics during simulated gastric digestion were observed by measuring particle size distributions, structuring at various length scales, as well as by evaluating differences in protein breakdown. Immediately after contact with the simulated gastric fluids, all samples showed extensive aggregation and formation of different structures. MPC control dispersions (no polysaccharide) and MPC containing alginate formed large inhomogeneous aggregates. The lack of structural homogeneity affected the simulated gastric emptying: there were marked differences in the type of aggregates present at various times of emptying depending on the hydrocolloid present in the mixture. MPC containing pectin or guar gum formed macroscopically homogeneous dispersion, with rather small protein aggregates showing a large population of particles between 60 and 100 μm of diameter, with marked differences in microstructure. Pectin created large coacervates, while guar microscopic phase separated systems. These dispersions showed a higher extent of protein digestion, due to the larger surface area created for enzyme activity compared to the macroscopically phase separated matrices. In all cases, there was a large undigested fraction at the end point of 140 min. SDS PAGE demonstrated differences in the casein peptides distribution depending on the type of polysaccharide present during simulated gastric emptying. This in spite of similarities in cumulative protein emptied. It was concluded that in this semi-continuous *in vitro* gastric digestion model, structuring with polysaccharides has a significant impact on gastric emptying and protein digestion kinetics.

1. Introduction

Characterization of the behavior and structure of various foods during gastrointestinal transit is important to clarify the role of food in human nutrition. It is becoming increasingly clear that the structure of the food regulates its disruption during digestion, affecting gastric empting, hormonal responses and absorption of the nutrients (Marciani et al., 2013; Mulet-Cabero et al., 2019). Mechanistic investigations on the relationships between the physical and chemical properties of the food matrix, and its subsequent behavior in the gastrointestinal tract, are needed. Such data can help enlighten how to develop food products with targeted nutritional properties, for example, to create satiety promoting functions, or to improve delivery and absorption of nutrients.

The structuring of food during digestion impacts nutrient absorption (Boutrou et al., 2013; Fardet et al., 2019; Guo et al., 2020). Studies showed that a steady release of nutrients during gastric emptying can affect satiety differently than the same meal consumed in a solid state (Marciani et al., 2012) causing delayed gastric emptying in healthy subjects. The physico-chemical mechanisms behind structuring of the food matrix in the gastric phase, modifying the kinetics of nutrient release are not fully revealed by intervention studies. Reliable tools are needed to enable these investigations.

Using semi-dynamic *in vitro* models makes it possible to follow the fate of the nutrients during gastric transit (Mulet-Cabero et al., 2020). For

* Corresponding author. 48 Agro Food Park, Aarhus N, 8200, Denmark.
E-mail address: mc@food.au.dk (M. Corredig).
[1] Contributed equally to the research.

https://doi.org/10.1016/j.crfs.2021.03.012
Received 9 November 2020; Received in revised form 28 March 2021; Accepted 29 March 2021

Table 1
Overview of sampling times and volumes during the semi continuous *in vitro* gastric digestion. The four gastric intervals (GI) were followed by an end point (END). Every GI consisted of two gastric emptying (GE) points of 92.4 mL each.

Gastric interval sample	Gastric emptying point	Emptying Time (min)	Actual gastric volume (mL)	Total volume Secreted (mL)
		0.0	458*	0.00
GI1	GE1	17	407	42.2
	GE2	33	356	83.4
GI2	GE3	50	305	125
	GE4	67	254	166
GI3	GE5	83	203	208
	GE6	100	153	250
GI4	GE7	117	102	291
	GE8	133	50.8	333
END	GE9	150	0.00	374

example, it was recently demonstrated that different dairy matrices, with same caloric content but varying in structure behavior during gastric digestion affect the kinetics of nutrient release, and likely change their bioaccessibility. For example, creaming or phase separation in the gastric phase generates a lower level of nutrients release in the intestine at the early stages of digestion (Mulet-Cabero et al., 2017; Ye et al., 2016).

Hydrocolloids are known to impart different viscoelastic properties to the food matrix, and to affect structuring dynamics during processing. This is also the case during disruption of the food matrix in the gastrointestinal tract. It has been suggested that ingestion of guar gum and alginate increases satiety and decreases food intake short-term. These effects are underpinned by the structuring dynamics occurring in the stomach (Paxman et al., 2008; Rao et al., 2015). An *in vivo* trial showed that a mid-morning snack of yoghurt enriched with hydrolyzed guar gum was able to significantly reduce appetite compared to non-enriched yoghurts, resulting in a lower energy intake during *ad libitum* lunch (Lluch et al., 2010).

The interactions between proteins and polysaccharides cause structuring in food matrices, and are driven by the structural features of the biopolymers, such as size, conformations, and charge densities. Alginate and pectins are anionic polysaccharides which have been shown to affect the breakdown on milk proteins during digestion (Koutina et al., 2018). Alginate consists of unbranched block-wise monomers of β-D-mannuronic acid and α-L-guluronic acid residues. The physical properties of alginate, such as gelling ability, gel strength, and viscosity, are strongly related to the ratio between the different sugar residues (Draget et al., 1997). Gelation of alginate can be induced by the acidic environment of the stomach (pH < 3.5), and/or the presence of calcium ions (Koutina et al., 2018). Pectin is composed of β-1,4-linked D-galacturonic acid residues, where the acidic carboxyl groups are esterified to various extents. The pectin in this study was a high ester pectin with a degree of esterification of around 70% and with a molecular structure fit for complexing with protein at low pH, thereby preventing development of large protein aggregates. Although the overall molecular charge density of this pectin was lower than for the alginate, this may not be the case in specific locations of the pectin molecule. While the pH of the medium has a significant impact on the charge densities of alginate and pectin, due to the changes in the protonation of the carboxyl groups, guar gum is neutral, and generally unaffected by changes in pH or ionic conditions (Wang et al., 2000). Guar is composed of neutrally charged galactomannans, made of a 1,4-linked β-D-mannopyranose backbone with 1,6-linked α-D-galactopyranosyl residues as side chains. These polysaccharides were used in the study to design marked differences in the structuring of the milk protein dispersions during gastric transit.

The complex formation of protein and polysaccharides can cause changes in the digestibility of proteins. For example, the *in vitro* digestibility of caseins or whey protein can be modulated by the presence of various polysaccharides (Koutina et al., 2018; Lamghari et al., 2000). This work aims, for the first time, to compare the behavior of milk protein concentrates structured by three different polysaccharides, during gastro intestinal transit using a semi dynamic *in vitro* model. Different structures were obtained by the addition of three different polysaccharides, namely, alginate, pectin and guar gum, and their structures were related to changes in protein breakdown, using a consensus *in vitro* semi-dynamic digestion model (Mulet-Cabero et al., 2020).

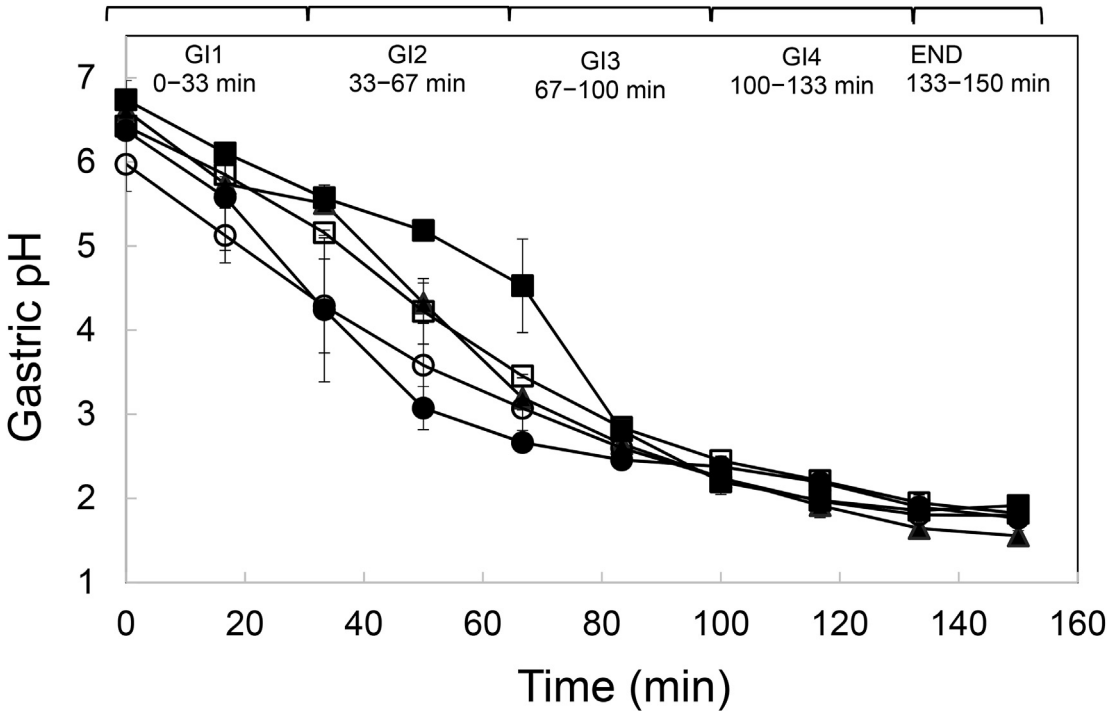

Fig. 1. pH changes, as a function of time, during gastric digestion of 3% Milk protein concentrate dispersions (filled circles), containing 1% alginate (filled triangles), 1% pectin (empty circles), 1% guar gum (filled squares), 0.5% alginate or 0.5% pectin (empty squares). Gastric intervals are indicated on top. Each data point is the result of two independent experiments. Bars indicate standard deviations.

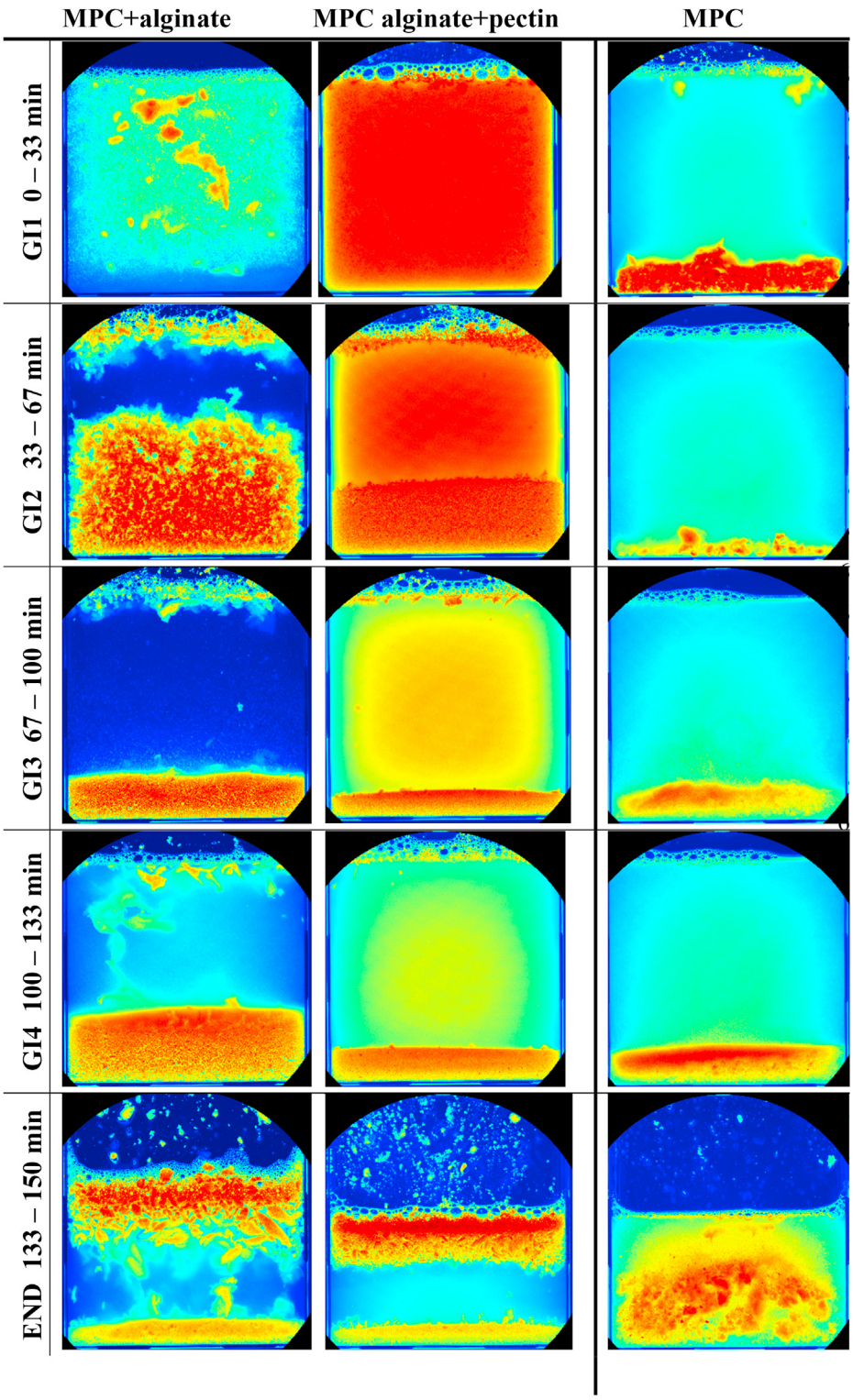

Fig. 2. Representative images collected using Videometer Liq for 3% MPC dispersions, control, or containing 1% alginate (MPC+alginate), or 0.5% alginate and 0.5% pectin (MPC+alginate+pectin). Different gastric intervals are indicated on the left axis. Last image is END point.

2. Materials and methods

2.1. Reagents

All chemicals were standard analytical grade and purchased from Sigma-Aldrich (Merck Life Sciences, Søborg, Denmark), unless otherwise indicated. Ultrapure type I water generated by a Milli-Q® system. Hemoglobin from bovine blood (H2500), Pepsin from porcine gastric mucosa (P7012) were also purchased from Sigma-Aldrich.

2.2. Food matrix preparation

Five different matrices were prepared by mixing equal volumes of a 6% (w/v) Milk protein concentrate solution (MPC) (Promilk 852A, 85%,

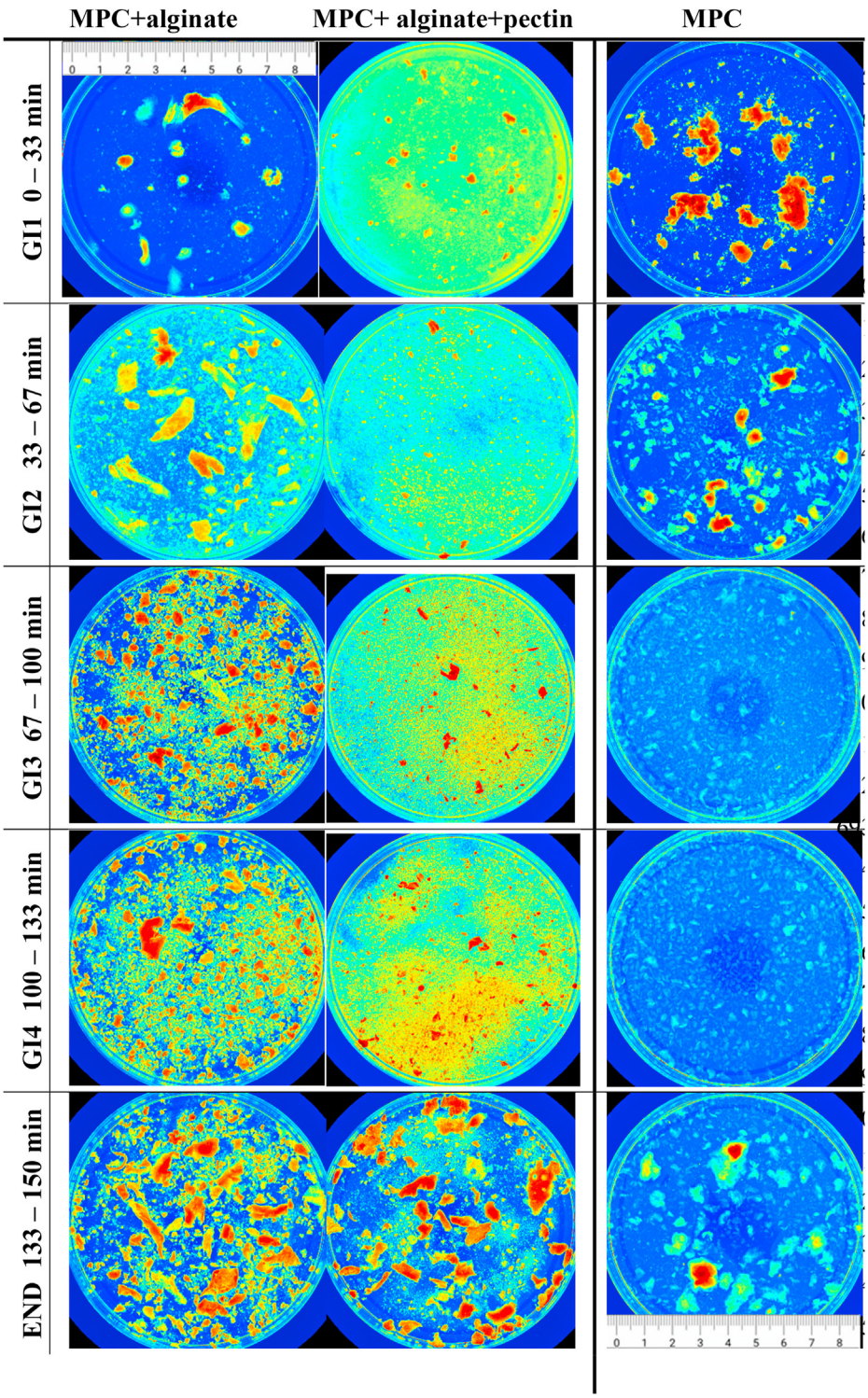

Fig. 3. Representative images of milk protein aggregates for 3% MPC dispersions, control (MPC), with 1% alginate (MPC+alginate) or with 0.5% alginate and 0.5% pectin (MPC+alginate+pectin).

Ingredia, Arras, France), and a 2 (w/v) solution of different polysaccharides, namely sodium alginate (Protanal 120RF, viscosity 400–600 mPa × s, medium gel strength, acid-sensitive properties and produced from Norwegian brown seaweed, Dupont, Nutrition and Biosciences, Aarhus, Denmark), pectin (GRINDSTED® Pectin 1387, non amidated, high ester Dupont), alginate and pectin (1:1 wt ratio), and guar gum (GRINDSTED® Guar 250, Dupont). A control dispersion containing only 3% (w/v) MPC was also prepared.

The polysaccharide (4.5 g) was dispersed in deionized water (225 mL) at room temperature with a high-speed overhead stirrer (2000 rpm, 10 min) followed by mixing for 90 min at lower speed (approximately 1000 rpm). The MPC (13.5 g) was dissolved in deionized water (225 mL) at 22 °C by high-speed overhead stirring (1000 rpm, for approximately 1.5 h) before mixing with the polysaccharide. The dispersions were then mixed, and 400 mL aliquots were preheated to 37 °C before subjecting them to digestion experiments.

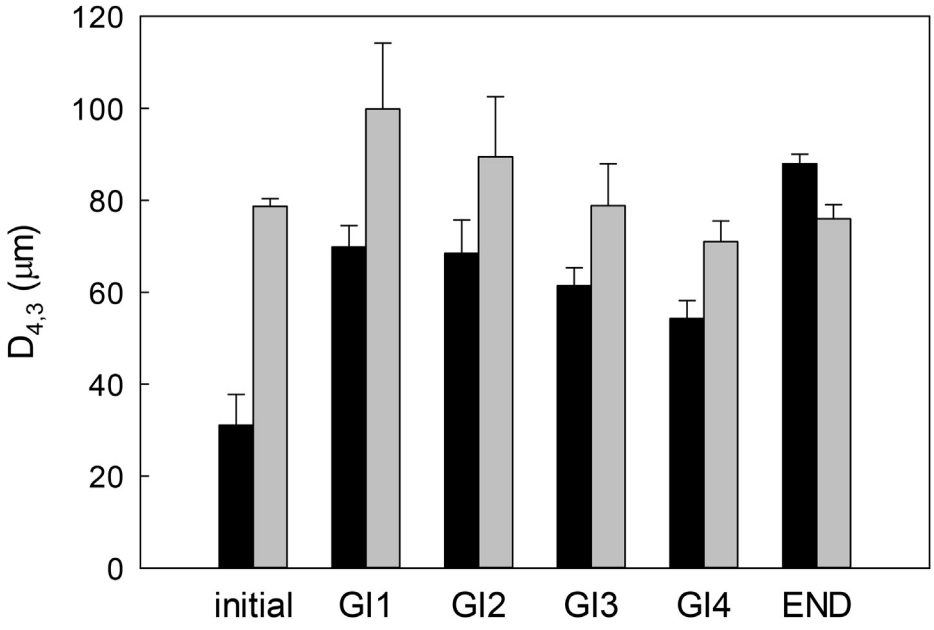

Fig. 4. Average particle size (D4,3) measured in the fractions emptied at various intervals, for MPC suspensions containing 1% pectin (black bar) or 1% guar gum (grey bar). Samples are the average of two separate digestion experiments. Bars indicate standard deviations.

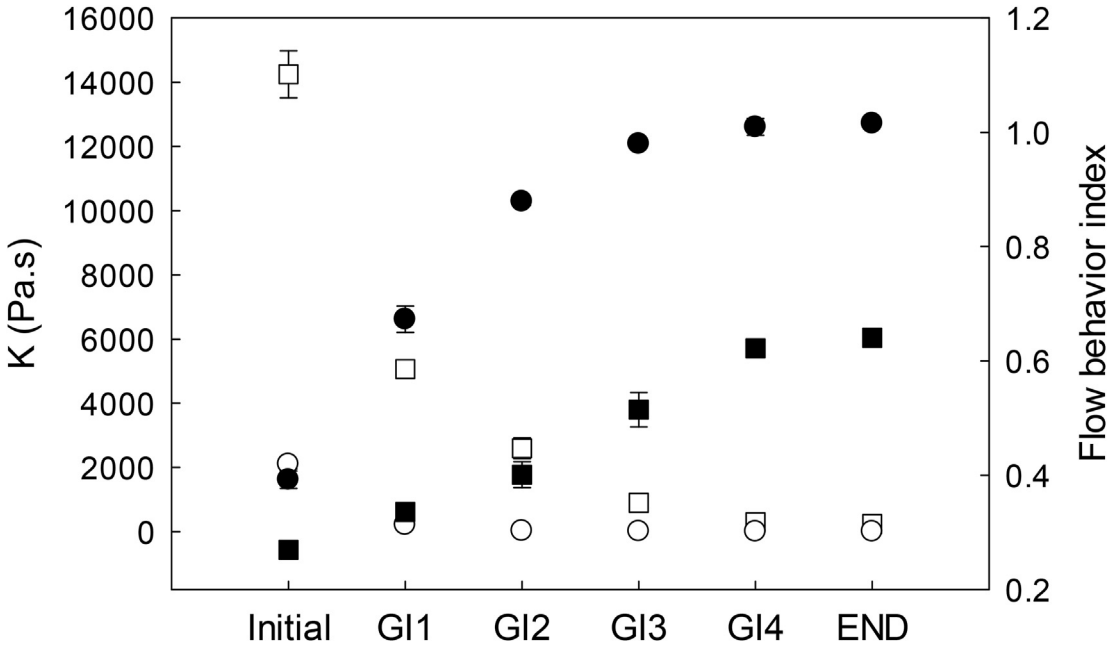

Fig. 5. Consistency index (K, empty symbols) and flow behavior index (filled symbols) for fractions emptied at various intervals, including initial and END point, measured by rheology, for MPC suspensions with 1% pectin (circles) and 1% guar gum (squares). Bars indicate standard deviations.

2.3. Simulated salivary and gastric fluid preparation

For the oral and gastric stage, a 1.25 × concentrated electrolyte simulated salivary and gastric fluid (SSF and SGF) solutions were prepared. The pH was adjusted to 7.00 with HCl. Immediately before use, the SSF and SGF were diluted with water, $CaCl_2$, enzyme solutions and HCl (1.5 M) to obtain final concentrations containing 15.1 or 6.90 mmol/L KCl, 3.70 or 0.90 mmol/L KH_2PO_4, 13.6 or 25.0 mmol/L $NaHCO_3$, 0.15 or 0.12 mmol/L $MgCl_2$, 0.06 or 0.5 mmol/L $(NH_4)_2CO_3$, 1.5 or 0.15 mmol/L $CaCl_2$, for SSF and SGF, respectively as previously reported[17]. Furthermore SGF contained a final concentration of 47.2 mmol/L NaCl. Pepsin (374.5 mg, activity: 4443 U/mg) was also prepared in the concentrated SGF (50.0 mL) solution to reach a final concentration of 4000 U/mL in the total SGF/pepsin solution volume (416 mL). The stomach vessel, the SSF, the SGF, the pepsin solution and the food matrix were preheated at 37 °C.

2.4. In vitro digestion

The *in vitro* oral and gastric digestion were carried out following semi-dynamic *in vitro* digestion protocol (Mulet-Cabero et al., 2020; Brodkorb et al., 2019) using a bioprocess controlled station (BioFlo® 120 bioprocess control station, Eppendorf; Merk Life Sciences). The gastric digestion vessel consisted of a 1 L glass vessel equipped with a 3D-printed

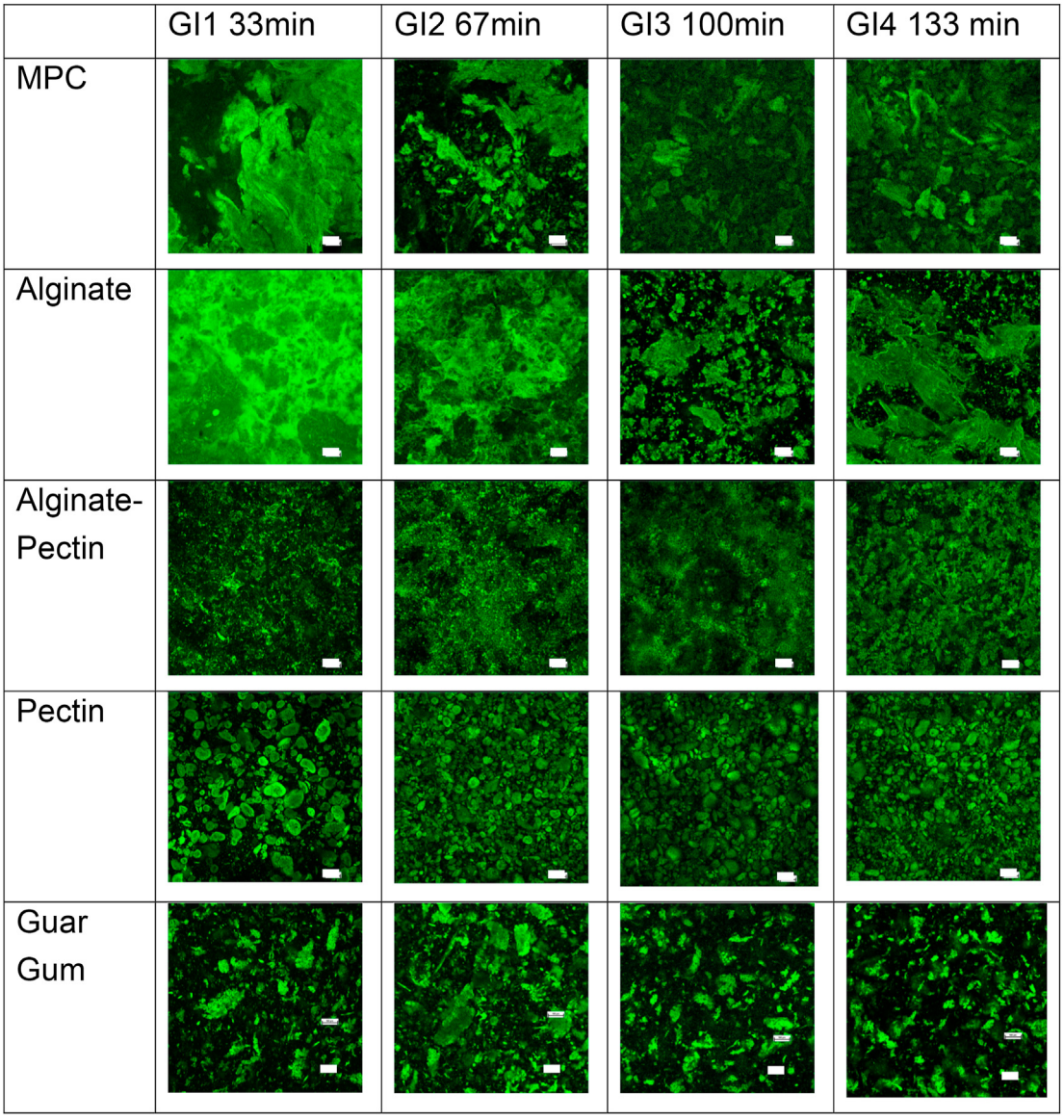

Fig. 6. Examples of confocal microscopy images of samples at various emptying intervals for MPC, MPC+alginate, MPC+alginate+pectin, MPC+pectin and MPC+guar. The scale bar corresponds to 100 μm. Light (green on web version) color represents the protein signal. (For interpretation of the references to color in this figure legend, the reader is referred to the Web version of this article.)

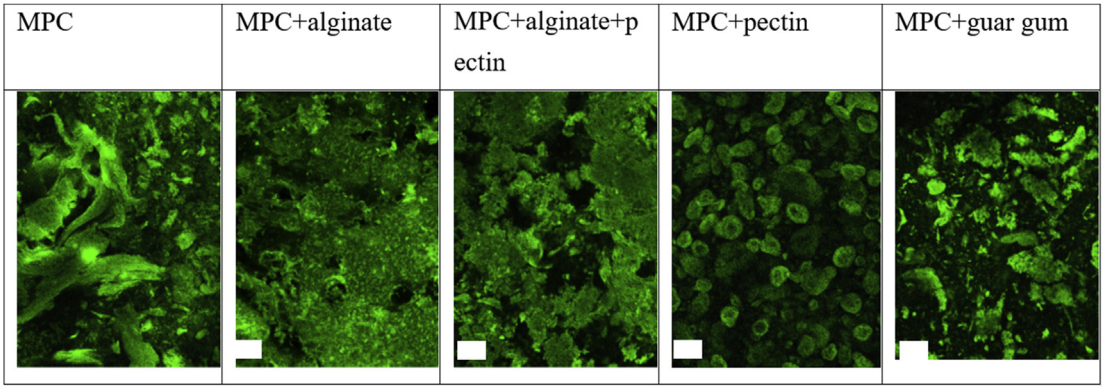

Fig. 7. Examples of confocal microscopy images of the digestates at END point for MPC, MPC+alginate, MPC+alginate+pectin, MPC+pectin, MPC+guar. The scale bar corresponds to 100 μm. Light (green on web version) color represents the protein signal. (For interpretation of the references to color in this figure legend, the reader is referred to the Web version of this article.)

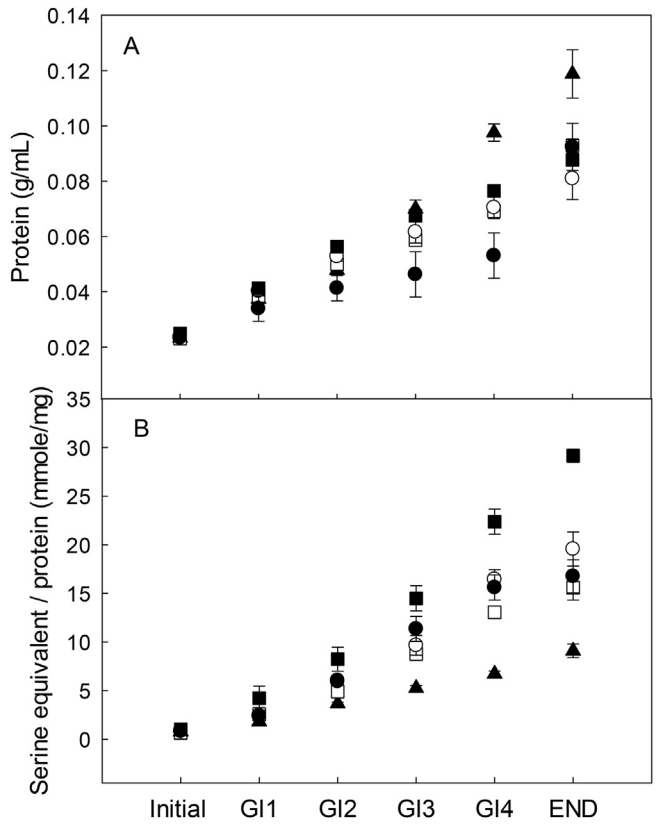

Fig. 8. Concentration of protein in the digesta (A), and free amine groups (serine equivalent) per mg of protein (B) at the various stages of gastric emptying for 3% Milk protein concentrate dispersions (filled circles), containing 1% alginate (filled triangles), 1% pectin (empty circles), 1% guar gum (filled squares), 0.5% alginate or 0.5% pectin (empty squares). Each data point is the average and error bars represent the standard deviation of two independent replicates.

stirring paddle, designed so that the paddle moves close to the bottom of the vessel and at the edge, leaving an approximately 6 mm of space between the paddle and the glass in the center, to allow for sampling. A ring shaped dispenser (6 mm outside diameter, Parflex 98, Parker Corp. Ravenna, OH, USA) was built to deliver the simulated gastric fluid through multiple holes <0.5 mm around the vessel. The ring was positioned initially just below the top surface of the food matrix, to deliver the SGF from multiple positions on the side and the top of the matrix. The SGF was distributed at 2.5 mL/min. The vessel temperature was controlled with a heat blanket and a water bath set at 37 °C. Continuous pH measurements were carried out with a pH meter (Ingold/Mettler Toledo) slightly higher than the paddle. Sampling was carried out at the bottom of the vessel using a 10 mL plastic pipette attached to a tip with an opening of 2.9 nm.

The amount of HCl required to bring the pH of the tested food to the final pH was estimated as previously reported (Mulet-Cabero et al., 2020). In brief, 400 mL of each food matrix was pre-warmed at 37 °C, SSF (16 mL) was added to the food matrix (400 mL, 16 g solids), and incubated with continuous stirring (2 min, 37 °C). The SSF was added at a 1 mL SSF per g of solids (Mulet-Cabero et al., 2020). The vessel lid equipped with the pH meter, the stirring paddle, the ring fluid dispenser (primed with SGF and the pepsin solution) and the heat blanket thermostat were placed on top of the stomach vessel.

In the vessel, the SGF was mixed with the food matrix-SSF. The initial mixture contained the oral mixture (400 mL of sample and 16 mL of SSF) + basal volume SGF (41.6 mL). The final volume of SGF added to the mix was equivalent to the volume of food mixed with the salivary fluid SSF (1:1 vol ratio to a total end-volume of matrix + secreted SGF of 832 mL) over the course of the gastric digestion phase (2.5 hours). During the simulated gastric digestion experiments, pepsin was pumped together with SGF just before being infused into the stomach vessel, to avoid autolysis of the pepsin. This was confirmed by preliminary tests ensuring no changes to enzyme activity upon dilution. The SGF (324.4 mL) and pepsin solution (50.0 mL) were continuously added at 2.16 and 0.333 mL/min, respectively. The pH was then slowly adjusted, under stirring, to pH 2.5 using 1.5 M HCl. The total volume needed to reach the final gastric pH was 19.5 mL for MPC, 20 mL for guar gum and pectin MPC dispersions, 22 mL for alginate and pectin MPC dispersions, and 27 mL

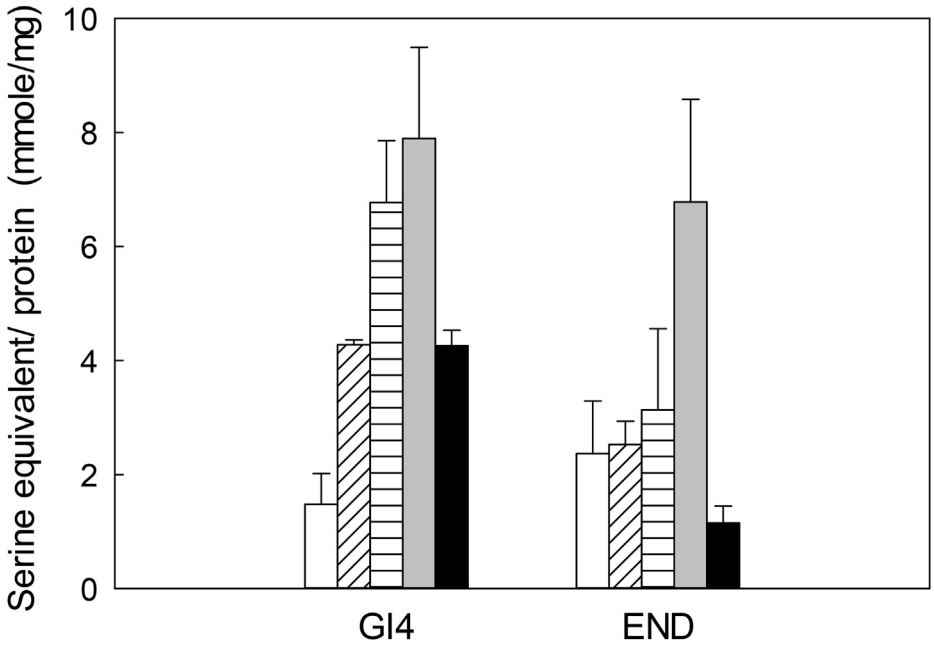

Fig. 9. Free amine groups (serine equivalent) per mg of protein measured in the digesta at GI4 and END point, for MPC control (black bars), MPC+alginate (white bars), MPC+alginate+pectin (diagonal bars), MPC+pectin (horizontal bar), MPC+guar (grey bar). Each data point is the average and error bars represent the standard deviation of two independent replicates.

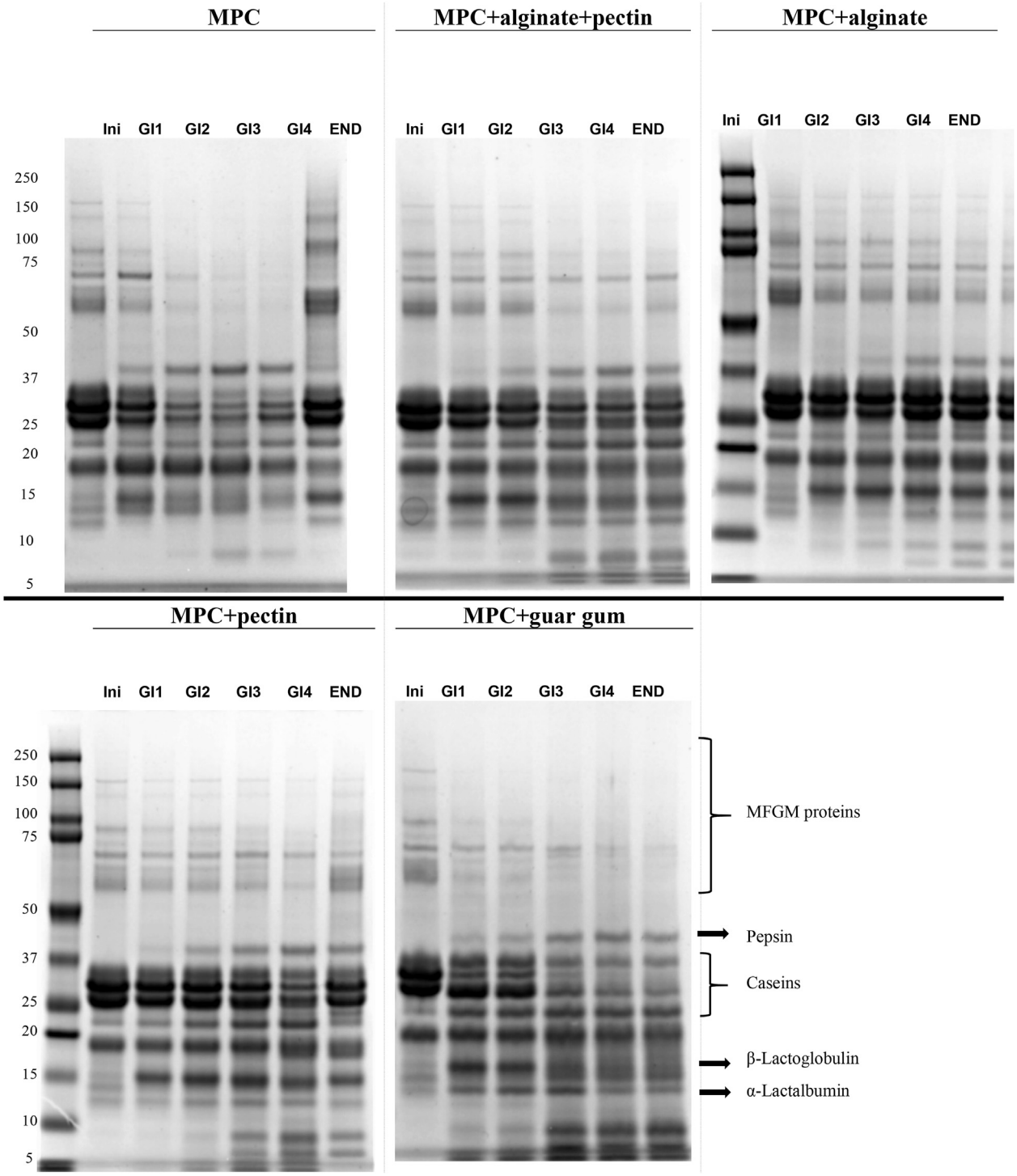

Fig. 10. SDS-PAGE analysis, based on protein, of the gastric digesta at the various stages of the *in vitro* digestion for MPC, MPC+alginate, MPC+alginate+pectin, MPC+pectin, MPC+guar, at different gastric emptying intervals. A set of standard marker proteins from 5 to 250 kDa is show in the left. Initial samples, GI gastric interval from 1 to 4, and END point.

for alginate MPC dispersions. The kinetics of acidification were then monitored during the *in vitro* digestion experiments, as these quantities did not consider the effect of emptying over time or the phase separation and stratifications that occurred in the various treatments.

2.5. Gastric emptying and sampling

During the entire duration of the *in vitro* digestion, emptying was carried out every 17 min by extracting 92.4 mL from the bottom of the vessel. The emptying times and volumes are summarized in Table 1. Each gastric interval (GI) consisted of two gastric emptying points. The end point (END) was taken by opening and emptying the vessel. While pectin+ MPC and guar+MPC remained macroscopically homogeneous during acidification, the other three matrices, alginate+pectin+MPC, alginate+MPC or MPC, created a phase separated unhomogeneous mass in the vessel.

Immediately after extraction, the samples were neutralized with NaOH (1 M) to pH 5–5.5 to inhibit most of the pepsin activity. The

samples were not neutralized completely to avoid the disruption of structures. The samples for structure characterization were kept refrigerated (4 °C) and rheology, confocal laser scanning microscopy and particle size analyses were performed within 48 h from digestion.

For protein analysis, representative samples from the four gastric intervals were neutralized with NaOH (1 M) to a pH above 8, to inactivate pepsin, and the samples were homogenized (25000 rpm, ~30 s, T25 Ultra-Turrax®, IKA®) and immediately frozen and kept at −23 °C. The same procedure was performed with undigested (initial) samples.

2.6. Visual observations

Visual analysis of the gastric samples was carried out using VideometerLiq and VideometerLab multispectral imaging instruments (Videometer A/S, Herlev, DK), shortly after the gastric digestion experiment. The digestates were left to settle in flasks (Sarstedt T-75 Cell Culture Flask) and then observed with a VideometerLiq (Videometer) at 365 nm. They were also placed on petri dishes and gently drained, and then suspended in purified water. In this case, the sediments were observed with a VideometerLab (Videometer) at 375 nm. Samples of MPC+pectin and MPC+guar did not show phase separation and therefore were not analyzed with this technique, but by using integrated light scattering. The raw pictures were colored with a "jet color scale", colors from blue to red, illustrating increase in aggregate density.

2.7. Confocal laser scanning microscopy (CLSM)

The microstructures of the initial and digested samples were analyzed by confocal laser scanning microscopy (CLSM) using a Nikon motorized spectral confocal microscope model Ti-E (DFA instruments, Glostrup, DK). The protein fraction in the digestate was labeled with fluorescein isothiocyanate (FITC, Merks Biosciences). The FITC was dissolved in acetone, and smeared evenly over a microscope glass and allowed to dry. The sample was gently placed on the microscope glass and the dye was allowed to absorb into the sample for minimum 30 minutes before microscopy. All the images were taken using a 10 × objective and an Argon laser at an excitation wavelength of 488 nm.

2.8. Particle size distribution

Particle size distribution of the gastric digestates was measured using laser light scattering (Mastersizer, Malvern Instruments, Malvern, UK). The measurements were only performed on visually homogeneous matrices (MPC+pectin and MPC+guar suspensions). Particle size distributions were recorded as volume weighted ($d_{4,3}$) means. Each measurement was carried out in duplicate.

2.9. Rheological analysis

In the case of MPC+pectin and MPC+guar dispersions, it was possible to measure their rheological properties, as all emptying points appeared homogeneous. Initial dispersions and the digestates at the various GI were gently loaded in a cup/bob geometry (Cylinder B-CC27, Physica MCR 301, Anton Paar) and measured at 37 °C using a rheometer (Physica MCR 301, Anton Paar). A short strain sweep (20 s) was conducted at very low strain percentages (0.1–1%), followed by a flow curve measurement, calculating viscosities over a broad range of shear rates (0.01–100 s^{-1}). Using the obtained flow curve data, the viscosity (η) was plotted as a function of shear rate ($\dot{\gamma}$) on logarithmic scales ($\log(\eta)$ vs. $\log(\dot{\gamma})$ plot for each GI-sample). Linear regressions were made on the linear part of these logarithmic plots according to the power law viscosity model, to calculate the flow behavior index (n) and the consistency index (K).

2.10. Degree of proteolysis

The extent of proteolysis was measured for all gastric interval samples using the o-phtaldialdehyde (OPA) assay (Nielsen et al., 2001). A buffer containing $Na_3PO_4{\cdot}12H_2O$ (15 g/L) and $CH_3(CH_2)_{11}OSO_3Na$ (SDS, 1 g/L) was prepared in deionized water and adjusted to pH 11 with HCl. A o-phtaldialdehyde (OPA) solution was prepared by dissolving 0.04 g/mL in EtOH. A DTT-solution containing dithiothreitol at 0.044 g/mL was prepared in deionized water. At the time of use, an OPA-reagent-solution (50 mL) was prepared by mixing the OPA-solution (1 mL) and the DTT-solution (1 mL) with the SDS Phosphate buffer (48 mL). The OPA-reagent-solution was protected from light and used immediately.

Aliquots of gastric samples (850 μL) were pretreated with 150 μL of 20% trichloroacetic acid solution, to cause protein precipitation. The samples were centrifuged (17000 g, 20 min, 22 °C) and the supernatant was removed, and centrifuged again (17000 g, 5 min, 22 °C). Supernatants (25 μL) were mixed with the OPA-reagent-solution (175 μL) in a microtiter plate, and after 50 min of incubation, the absorbance was measured at 340 nm and subtracted from controls prepared with water. The data were measured against a standard curve prepared with Serine (0.07–4.7 mM) and reported as released serine equivalents per mg of protein.

The protein concentration was measured using the Dumas method using a DUMATHERM® nitrogen analyzer (Gerhardt Analytical Systems, Königswinter, Germany). A conversion factor of 6.38 was used to obtain the protein content from the nitrogen content.

2.11. Protein digestion measured by SDS-PAGE

SDS-PAGE analysis was conducted on the various digesta samples as well as the initial undigested matrices, after dilution of all samples to 0.5% protein in milliQ water and then further diluted 1:2 in 0.1 mol/L Na-phosphate buffer, pH 7.0. The samples were then mixed 1:1 with 2 × Laemmli sample buffer (20 μL) containing DTT (350 mmol/L) and placed on a heat block (80 °C, 4 min). Protein standards (10 μL, Precision Plus Protein™ Dual Xtra #1610377, BIO-RAD) and the test samples (20 μL) were loaded onto a NuPAGE™ 4–12% Bis-Tris gel (10 well, 1.0 mm, Invitrogen™). Dithiothreitol 99% (DTT, 457779, Sigma-Aldrich), 2x Laemmli Sample Buffer (BIO-RAD, #1610737), NuPAGE™ 4–12% Bis-Tris gel 10 well 1.0 mm (Invitrogen™), NuPAGE™ MOPS SDS Running Buffer (20x, Invitrogen™), Precision Plus Protein™ Dual Xtra (BIO-RAD, #1610377), SimplyBlue™ SafeStain (Invitrogen™). The electrophoresis (40 min, 200V, 120 mA [240 mA for 2 gels], 25W) was performed using NuPAGE™ MES SDS running buffer. The gel was rinsed two times in water, followed by staining with Invitrogen™ SimplyBlue™ SafeStain (60 min, 22 °C). The gel was de-stained in water (100 mL, 1 hour). A NaCl solution (20% w/v, 20 mL) was added to the de-staining water and the gel was incubated overnight. Gel Imaging were performed on a Gel Doc™ EZ System (BIO-RAD) using Image Lab™ software.

3. Results and discussion

3.1. Structure formation during gastric digestion

The amount of oral and gastric juices to be added to the mixture was derived from the INFOGEST recommendations, whereby a 1:1 ratio of SSF was added based on solids, and then, this mixture entered the gastric vessel already containing 10% of the total SGF volume. The pH will then decrease gradually from an initially high level, due to the buffering capacity of the protein, to a final pH of 2. Different amounts of HCl were added to the mixtures to account for the differences in buffering capacity of the polysaccharide molecules. The pH profiles of the various mixtures are shown in Fig. 1. There were some differences in the first part of the digestion, for the mixtures containing guar gum (Fig. 1, filled squares), as well as those containing alginate, and alginate and pectin. The higher values for guar gum at the initial stages of mixing were due to the more homogeneous protein distribution in the mixture and the higher viscosity of the continuous phase compared to the other systems, slowing down migration of acid to the pH electrode through the mixing.

In MPC control dispersions (Fig. 1, filled circles), values dropped to pH around 3 after 45 min of digestion. This was due to the inhomogeneous structure, which caused a high discharge of protein at the initial stages of gastric emptying (small particles, precipitated at the bottom of the vessel) in combination with the continuous addition of SGF in the vessel. The presence of inhomogeneous aggregated structures in MPC confirmed prior *in vivo* observations (Fletcher et al., 2001; Hila et al., 2006).

The visual appearance of these suspensions at various stages of gastric emptying are shown in Figs. 2 and 3. Fig. 2 illustrates difference in the nature of the precipitates present at the various gastric interval (GI) points, while Fig. 3 compares the size of the large aggregates present in MPC, and MPC+alginate and MPC+alginate+pectin digestates, at the various emptying stages. The samples containing guar and pectin are not shown, as they were homogeneous and showed very small aggregates, which were instead characterized by integrated light scattering (Fig. 4).

In the case of MPC and MPC containing alginate or alginate+pectin (Figs. 2 and 3), precipitates made up of large aggregates were present at all gastric emptying points. Furthermore, in all cases, large aggregates were also present at the end point after 2.5 h of gastric digestion. From the initial stage to GI4, there was a clear decrease in the amount of precipitate present in the emptied fractions. In the MPC control, rigid and large particles were present at the END point (Figs. 2 and 3). A difference from GI4 to END is expected, as the end point will collect all the residual material left after digestion, while the first 4 gastric emptying interval points were sampled from the bottom of the gastric vessel. The MPC control formed aggregates immediately, due to the pH value already below 6 once mixed with SGF mixture, as well as the presence of pepsin and local areas which may have considerably lower pH values. The aggregation of casein protein in the gastric environment has previously been described as a mixed aggregation caused by proteolysis and pH destabilization (Ye et al., 2016).

The MPC+alginate contained the largest precipitates, compared to MPC control or MPC+pectin+alginate. The effect of alginate on the presence of large, undigested aggregates is obvious looking at the END points in Figs. 2 and 3. Also in the case of MPC dispersions with alginate and alginate+pectin, the dispersions entered the vessel as pourable, homogeneous matrices, and immediately aggregated upon contact with the SGF. In this case, the aggregation was not only mediated by acid and pepsin, but also the presence of calcium ions, present in the SGF, as well as released by the casein micelles during acidification (Li and Corredig, 2019). The structures were gradually disrupted within the first 60 min of *in vitro* digestion, due to dilution with the SGF and mixing. At the first emptying point (GI1) the MPC+alginate matrix appeared to have some large aggregates suspended in a viscous matrix (Fig. 2), at this time, most aggregates were still too large to pass through the *in vitro* emptying stage. Subsequent emptying points showed an increase in the precipitation, with a gradual decrease in the aggregate size, as shown in Fig. 3. The MPC+alginate+pectin suspensions formed smaller structures than those of MPC+alginate (Figs. 2 and 3). In all cases, the END points still presented large inhomogeneous structures.

Unlike the MPC control dispersion, and those containing alginate, the 3% MPC with pectin or guar gum had a macroscopically homogenous appearance. It was then possible to analyze their particle size by light scattering, as shown in Fig. 4. The average apparent particle diameter increased from initial to the first gastric emptying point (GI1) in both treatments. In general, MPC+pectin showed a smaller average particle size than MPC+guar, and, in the case of guar gum, there was a decrease in particle size over gastric emptying time. Both suspensions at the END point showed an average particle diameter (D4,3 of about 80 μm).

Due to the homogeneous appearance of these two treatments, the viscosity was also measured in the MPC dispersions containing pectin or guar gum, at various stages of *in vitro* gastric emptying, as shown in Fig. 5. As shown by the initial values of the consistency index, both matrices entered the stomach as viscous liquids, with the suspension containing guar gum markedly more viscous than that containing pectin. The MPC+pectin dispersion showed a sharp drop in consistency index, immediately after gastric dilution and mixing, with a continuous decrease over the *in vitro* digestion. In contrast, the MPC+guar mixture displayed a more gradual decline in consistency index (due to the gradual dilution with SGF), showing a significantly higher viscosity throughout, compared to the MPC+pectin suspension. In both suspensions, the flow behavior index showed a marked increase over time, with pectin showing a more newtonian fluid behavior in the last phases of gastric digestion. On the other hand, MPC+guar suspensions showed flow behavior indexes <0.7 even at the END point, indicating a shear thinning structure throughout gastric digestion.

3.2. Microstructural changes during in vitro digestion

Examples of the microstructures observed for the different emptying time fractions, are shown in Fig. 6. MPC control dispersions showed large aggregated particles, decreasing in size over time. Aggregates larger than 100 μm were still observed in the last gastric emptying point. Both MPC+alginate and MPC+alginate+pectin were characterized by a clear protein network throughout the field of view, and mixtures containing both alginate and pectins showed smaller aggregates than those containing only alginate, or MPC control. Confirming visual observations, the MPC dispersions containing pectin or guar gum showed aggregation microscopically, but a homogeneous dispersion macroscopically, with protein aggregates markedly different in structure.

The first fraction emptied after 30 min of *in vitro* digestion, showed drastic differences between treatments, in terms of size and microstructure. During digestion, MPC+alginate suspension primarily formed large, low-density, porous structures. MPC control initially aggregated into large network structures, and the gel gradually was disrupted over time. The initial gel structure of MPC+alginate was largely preserved in GI1 and GI2. The presence of pectin in the MPC+alginate+pectin mixtures caused aggregation in significantly smaller particles and in a finer gel structures compared to MPC+alginate. In MPC mixtures containing pectin or guar gum, smaller micro-phase separated aggregates were present in the initial stages of gastric emptying and sizes slightly decreased over time. The aggregates were less than 100 μm in size, in agreement with the light scattering results reported in Fig. 4.

The confocal observations confirmed what expected from the functionality of this pectin (suited to stabilize acidified protein drinks), namely the ability to limit the aggregates size, by hindering the interaction between the small aggregates. As the pH of the caseins decreases, the negative charges of the pectin interact with the positive moieties present on the caseins, forming protein-polysaccharide aggregates. These coacervates formed between the protein aggregates and pectin sterically stabilized these structures and maintained a macroscopically homogeneus dispersion, which gradually decreased over time.

In the MPC+guar mixture, guar gum caused microscopic phase separation, due to the thermodynamic incompatibility between the guar gum molecules and the casein proteins, forming aggregates. Hence, small protein particle aggregates formed in the protein rich phases. In this case it was shown that the particle size decreased over time, also due to a contraction of the structures during further acidification, and increased hydrolysis. These differences in microstructure between MPC+pectin and MPC+guar were well aligned with the flow behavior characteristics shown in Fig. 5.

Fig. 7 compares all the END points for the *in vitro* gastric digestion. In all cases, large protein aggregates were still present. Due to the homogeneous distribution within the gastric vessel, the END points for MPC dispersions containing pectin or guar gum seemed to be similar to those shown in Fig. 6 for GI4.

3.3. Protein digestion

Fig. 8 shows the cumulative amount of protein measured during the gastric emptying (A) and the free amines released per mg of protein (B),

reflecting the extent of gastric proteolysis of MPC as a function of time. In all matrices, there was an increase in the amount cumulative amount of protein emptied, as well as a gradual increase in proteolysis.

Structuring with alginate (triangles) caused the highest level of protein measured in the fractions emptied, but with the lowest level of free amines in the digestates, compared to the other treatments. On the other hand, the MPC+guar dispersions (filled squares) showed the highest levels of free amines, especially at GI4 and END point. All other treatments showed similar values of protein during digestion (Fig. 8A) and intermediate levels of amine release. When compared to the other homogeneous dispersion, the data would indicate that, although the homogeneity of the suspensions and the small protein particle size caused a higher extent of digestion, the pectin-MPC was less accessed by the gastric enzyme, compared to MPC+guar dispersion. This is expected, as the coverage of the protein by the pectin causes a lower accessibility to the pepsin in the coacervate[22]. Fig. 9 shows the amount of serine equivalent measured at GI4 and the END point samples. The END showed significantly lower levels of free amines per mg of protein, demonstrating still the presence of undigested protein after 2.5 h of *in vitro* digestion. Only the MPC+guar mixture showed a consistent level of free amines at the END, compared to GI4, showing the homogeneous nature of the matrix. MPC samples (black bars), as well as those samples containing pectin showed significantly lower levels of serine equivalents at the END point compared to GI4, demonstrating large unhomogeneities.

To better identify possible differences in protein breakdown in the gastric stage, as a function of polysaccharide type, the protein composition at the various emptying points during the gastric phase was analyzed by SDS-PAGE (Fig. 10). The gastric digesta were compared at similar protein concentration, to better differences in the digestion pattern. The MPC suspension, before digestion contained all the major milk proteins, including the milk fat globule membrane proteins, caseins, and whey proteins. The protein bands were clearly different already after the first GI emptying point, in all cases, with higher ratios of whey proteins and caseins present in the emptied fraction. However, there were major differences in the breakdown pattern depending on the type of aggregates formed with the polysaccharides. In all cases, β-lactoglobulin seemed to be weakly affected by the gastric digestion compared to the other major proteins. This is in agreement with *in vivo* and *in vitro* data showing that the β-lactoglobulin mainly empties from the stomach as intact protein (Mahé et al., 1996; Villaume et al., 2004).

The caseins, as well as the high molecular weight bands associated with the milk fat globule membrane proteins tended to weaken going from GI1 to GI4, in nearly all matrices. However, the MPC+alginate showed high preservation of the casein from GI1 to END point. In the MPC control, protein emptied at the early stages, due to the precipitation and breakdown, allowing for a more diluted system overall at the later stages of the *in vitro* gastric digestion, and at GI4 point much less protein is present, indicating more hydrolysis, as all bands were loaded at the same protein level (as per nitrogen measurement). MPC+guar also showed a higher extent of hydrolysis at the end of the *in vitro* digestion. The results, albeit qualitative in nature, may also suggest differences in the casein accessibility.

The intensity decrease of the casein bands were accompanied by an increase in small molecular weight peptides. Marked development of small peptides (5–10 kDa) in GI3, GI4, and EPS, was observed for all matrices. The largest increase in small peptides was observed for MPC+guar during the gastric phase. The least casein breakdown was shown for MPC+alginate.

4. Conclusions

Gastric structuring using hydrocolloids is a valid strategy to modulate gastric digestion, as it modifies the microstructure of the aggregates and may cause delays in proteolysis. Different hydrocolloids were purposely chosen in this work in line with the known physico-chemical behavior and their ability to interact with proteins as a function of pH. In general, proteolysis levels decreased going from GI4 to END, indicating the effect of non homogeneous distributions of protein and aggregate sizes. The milk proteins present in the MPC control dispersions showed immediate precipitation in the presence of the gastric juices due to acidification and pepsin activity. However, in the presence of alginate, large particles were obtained and these coacervates made the protein less susceptible to pepsin hydrolysis. Macroscopically homogeneous suspensions were obtained with the addition of pectin or guar gum to the MPC dispersion. These systems showed that microstructural differences influenced by the specific polysaccharides can also modulate proteolysis kinetics. High ester pectin is known to maintain casein aggregates dispersed in acid environments. In this study, it was clearly shown that these coacervates were more resistant to proteolysis compared to the aggregates suspended in a microphase separated system formed by using guar gum.

In conclusion, by carefully designing the structures using their known physico-chemical properties and their ability to interact with proteins, it is possible to modulate the digestion behavior of the proteins at the gastric stage. The matrices prepared displayed large structural differences during gastric digestion, and these could be directly correlated to the measured variations in protein digestion. The presented methodology constitutes a powerful tool to understand food structuring and nutrient digestibility which can help to provide knowledge about the nutritional impact of various foods.

CRediT authorship contribution statement

Jacob Østergaard Markussen: Methodology, data collection, Data curation, Writing – original draft. **Finn Madsen:** Conceptualization, Data curation, advising, writing, Validation, Writing – review & editing. **Jette Feveile Young:** advising, Writing – review & editing. **Milena Corredig:** Conceptualization, Data curation, advising writing, Validation, Writing – review & editing.

Declaration of competing interest

The authors declare that they have no known competing financial interests or personal relationships that could have appeared to influence the work reported in this paper.

References

Boutrou, R., Gaudichon, C., Dupont, D., Jardin, J., Airinei, G., Marsset-Baglieri, A., Benamouzig, R., Tomé, D., Leonil, J., 2013. Sequential release of milk protein-derived bioactive peptides in the jejunum in healthy humans. Am. J. Clin. Nutr. 97, 1314–1323. https://doi.org/10.3945/ajcn.112.055202.

Brodkorb, A., Egger, L., Alminger, M., Alvito, P., Assuncão, R., Balance, S., Bohn, T., Bourlieu-Lacanal, C., Boutrou, R., Carriére, F., Clemente, A., Corredig, M., Dupont, D., Dufour, C., Edwards, C., Golding, M., Karakaya, S., Kirkhus, B., Le Feunteun, S., Lesmes, U., Macierzanka, A., Mackie, A.R., Matins, C., Marze, S., McClements, D.J., Ménard, O., Minekus, M., Portmann, R., Santos, C.N., Souchon, I., Singh, R.P., Vegarud, G., Wickham, M.S.J., Weitschies, W., Recio, I., 2019. INFOGEST static in vitro simulation of gastrointestinal food digestion. Nat. Protoc. 14, 991–1014. https://doi.org/10.1038/s41596-018-0119-1.

Draget, K.I., Skjåk-Bræk, G., Smidsrød, O., 1997. Alginate based new materials. Int. J. Biol. Macromol. 21, 47–55. https://doi.org/10.1016/S0141-8130(97)00040-8.

Fardet, A., Dupont, D., Riouz, L.E., Turgeon, S.L., 2019. Influence of food structure on dairy protein, lipid and calcium bioavailability: a narrative review of evidence. Crit. Rev. Food Sci. Nutr. 59, 1987–2010. https://doi.org/10.1080/10408398.2018.1435503.

Fletcher, J., Wirz, A., Young, J., Vallance, R., McColl, K.E., 2001. Unbuffered highly acidic gastric juice exists at the gastroesophageal junction after a meal. Gastroenterology 121, 775–783. https://doi.org/10.1053/gast.2001.27997.

Guo, Q., Ye, A., Singh, H., Rousseau, D., 2020. Destructuring and restructuring foods during gastric digestion. Compr. Rev. Food Sci. Food Saf. 19, 1658–1679. https://doi.org/10.1111/1541-4337.12558.

Hila, A., Bouali, H., Xue, S., Knuff, D., Castell, D.O., 2006. Postprandial stomach contents have multiple acid layers. J. Clin. Gastroenterol. Behav. Skim 40, 612–617. https://doi.org/10.1097/00004836-200608000-00010.

Koutina, G., Ray, C.A., Lametsch, R., Ipsen, R., 2018. The effect of protein-to-alginate ratio on in vitro gastric digestion of nanoparticulated whey protein. Int. Dairy J. 77, 10–18. https://doi.org/10.1016/j.idairyj.2017.09.001.

Lamghari, E., Kossori, R., Sanchez, C., El Boustani, E.S., Maucourt, M.N., Sauvaire, Y., Mejean, L., Villaume, C., 2000. Comparison of effects of prickly pear (Opuntia ficus

indica sp) fruit, Arabic gum, carrageenan, alginic acid, locust bean gum and citrus pectin on viscosity and in vitro digestibility of casein. J. Sci. Food Agric. 80, 359–364. https://doi.org/10.1002/1097-0010(200002)80:3<359::AID-JSFA534>3.0.CO;2-8.

Li, Y., Corredig, M., 2019. Acid induced gelation milk concentrated by membrane filtration. J. Texture Stud. 51, 101–110. https://doi.org/10.1111/jtxs.12492.

Lluch, A., Hanet-Geisen, N., Salah, S., Salas-Salvadó, J., L'Heureux-Bouron, D., Halford, J.C., 2010. Short-term appetite-reducing effects of a low-fat dairy product enriched with protein and fibre. Food Qual. Prefer. 21, 402–409. https://doi.org/10.1016/j.foodqual.2009.10.001.

Mahé, S., Roos, N., Benamouzig, R., Davin, L., Luengo, C., Gagnon, L., Gaussergès, N., Rrautureau, J., Tomé, D., 1996. Gastrojejunal kinetics and the digestion of [15N] beta-lactoglobulin and casein in humans: the influence of the nature and quantity of the protein. Am. J. Clin. Nutr. 63, 546–552. https://doi.org/10.1093/ajcn/63.4.546.

Marciani, L., Hall, N., Pritchard, S.E., Cox, E.F., Totman, J.J., Lad, M., Hoad, C.L., Foster, T.J., Gowland, P.A., Spiller, R.C., 2012. Preventing gastric sieving by blending a solid/water meal enhances satiation in healthy humans. J. Nutr. 142, 1253–1258. https://doi.org/10.3945/jn.112.159830.

Marciani, L., Pritchard, S.E., Hellier-Woods, C., Costigan, C., Hoad, C.L., Gowland, P.A., Spiller, R.C., 2013. Delayed gastric emptying and reduced postprandial small bowel water content of equicaloric whole meal bread versus rice meals in healthy subjects: novel MRI insights. Eur. J. Clin. Nutr. 67, 754–758. https://doi.org/10.1038/ejcn.2013.78.

Mulet-Cabero, A.I., Rigby, N.M., Brodkorb, A., Mackie, A.R., 2017. Dairy food structures influence the rates of nutrient digestion through different in vitro gastric behavior. Food Hydrocolloids 67, 63–73. https://doi.org/10.1016/j.foodhyd.2016.12.039.

Mulet-Cabero, A.I., Mackie, A.R., Wilde, P.J., Fenelon, M.A., Brodkorb, A., 2019. Structural mechanism and kinetics of in vitro gastric digestion are affected by process-induced changes in bovine milk. Food Hydrocolloids 86, 172–183. https://doi.org/10.1016/j.foodhyd.2018.03.035.

Mulet-Cabero, A.I., Egger, L., Portmann, R., Ménard, O., Marze, S., Minekus, M., Le Feunteun, S., Sarkar, A., Grundy, M.M.L., Carrière, F., Golding, M., Dupont, D., Recio, I., Brodkorb, A., Mackie, A., 2020. A standardised semi-dynamic in vitro digestion method suitable for food–an international consensus. Food Funct. 11, 1702–1720. https://doi.org/10.1039/C9FO01293A.

Nielsen, P., Petersen, D., Dambmann, C., 2001. Improved method for determining food protein degree of hydrolysis. J. Food Sci. 66, 642–646. https://doi.org/10.1111/j.1365-2621.2001.tb04614.x.

Paxman, J.R., Richardson, J.C., Dettmar, P.W., Corfe, B.M., 2008. Daily ingestion of alginate reduces energy intake in free-living subjects. Appetite 51, 713–719. https://doi.org/10.1016/j.appet.2008.06.013.

Rao, T.P., Hayakawa, M., Minami, T., Ishihara, N., Kapoor, M.P., Ohkubo, T., Juneja, L.R., Wakabayashi, K., 2015. Post-meal perceivable satiety and subsequent energy intake with intake of partially hydrolysed guar gum. Br. J. Nutr. 113, 1489–1498. https://doi.org/10.1017/S0007114515000756.

Villaume, C., Sanchez, C., Méjean, L., 2004. β-Lactoglobulin/polysaccharide interactions during in vitro gastric and pancreatic hydrolysis assessed in dialysis bags of different molecular weight cut-offs. Biochim. Biophys. Acta Gen. Subj. 1670, 105–112. https://doi.org/10.1016/j.bbagen.2003.10.017.

Wang, Q., Ellis, P.R., Ross-Murphy, S.B., 2000. The stability of guar gum in an aqueous system under acidic conditions. Food Hydrocolloids 14, 129–134. https://doi.org/10.1016/S0268-005X(99)00058-2.

Ye, A., Cui, J., Dalgleish, D., Singh, H., 2016. Formation of a structured clot during the gastric digestion of milk: impact on the rate of protein hydrolysis. Food Hydrocolloids 52, 478–486. https://doi.org/10.1016/j.foodhyd.2015.07.023.